JOURNAL OF VIROLOGY, Oct. 1999, p. 8640–8646 Vol. 73, No. 10
0022-538X/99/$04.00+0

In Vitro and In Vivo Characterization of a Mouse Adenovirus Type 1 Early Region 3 Null Mutant

ANGELA N. CAUTHEN,[1]† CORRIE C. BROWN,[2] AND KATHERINE R. SPINDLER[1]*

Department of Genetics, Franklin College of Arts and Sciences,[1] and Department of Veterinary Pathology, College of Veterinary Medicine,[2] University of Georgia, Athens, Georgia 30602

Received 7 May 1999/Accepted 16 June 1999

Previous attempts to construct a mouse adenovirus type 1 early region 3 (E3) null mutant by initiator codon mutagenesis were unsuccessful because one of the E3 proteins, gp11K, is synthesized as a fusion protein from a late viral mRNA (A. N. Cauthen and K. R. Spindler, Virology 259:119–128, 1999). Therefore, a different mutagenesis strategy was employed that inserted termination codons into all three reading frames of the E3 proteins. This strategy produced a mutant, *pm*E314, that was null for the expression of E3 proteins as determined by immunoprecipitation with E3-specific antisera. This mutant grew as well as wild-type (wt) virus in both 3T6 mouse fibroblasts and mouse brain microvascular endothelial cells. However, the 50% lethal dose for *pm*E314 in adult NIH Swiss outbred mice was approximately 6 log units higher than that of wt virus, indicating that *pm*E314 was less virulent in mice. In situ hybridization experiments revealed that the absence of the E3 proteins did not alter the tropism of the mutant virus from that of wt virus. When the histopathology was evaluated, the characteristics of the *pm*E314 infection at both doses administered were strikingly different from those exhibited by wt virus. The central nervous system of wt-infected mice exhibited damage to the endothelium and recruitment of inflammatory cells, whereas the central nervous system of *pm*E314-infected mice showed no inflammatory response and only mild signs of endothelial damage.

Mouse adenovirus type 1 (MAV-1) contains a double-stranded, linear DNA genome that is 30,944 bp in length (17). The organization of the MAV-1 genome is quite similar to that of human adenoviruses (hAds), but MAV-1 does not encode virus-associated RNAs (17). Early region 1 (E1), the late genes, and E3 are encoded on the top strand of the virus, while early region 2 (E2), early region 4 (E4), and IVa2 are encoded on the bottom strand of the virus.

The E3 region of MAV-1 is embedded in the cluster of late genes toward the right end of the genome. E3 mRNA transcripts at early times in infection are driven by a nearby promoter. Three mRNA species that are transcribed from this promoter are 5′ and 3′ coterminal, and each contains three exons and two introns. The first intron of each of the three mRNA species is spliced at the same donor and acceptor sites, so that when translated, these proteins share a common N-terminal sequence. However, the second intron of each is differentially spliced by using different combinations of donor and acceptor splice sites, giving rise to three unique C termini and thus potentially three unique proteins (1). To date, only one of the three E3 proteins, gp11K, has been detected in a wild-type (wt) infection in cell culture. This 14K protein is *N*-glycosylated and resides in the endoplasmic reticulum (ER) as a peripheral membrane protein (3).

gp11K is synthesized in infected cells by two mechanisms. Most of the protein produced in infected cells in culture is translated from an early mRNA species described above. However, a small amount of gp11K is translated from a late mRNA as a fusion between a late protein, likely the structural protein pVIII, and gp11K (5). Only the mature 14K-sized gp11K protein is detected in infections; therefore, we hypothesize that the fusion protein is cleaved at the gp11K signal sequence cleavage site to produce the mature 14K-sized gp11K protein that is localized to the ER.

Studies of MAV-1 acute infections in vivo have revealed that the virus causes neurological signs of disease in susceptible adult mice (11, 14). The clinical signs of disease and associated pathology have been determined in two mouse strains: NIH Swiss outbred mice (13, 14) and inbred C57BL/6 mice (11). The neurological signs of disease include ruffled coat, mild ataxia, and hunched posture and posterior paresis, followed by total flaccid paralysis and abdominal breathing (14). In situ hybridization and immunohistochemistry analysis showed that the major sites of MAV-1 infection in both NIH Swiss outbred and C57BL/6 mice are the endothelium of the brain and spinal cord and lymphoid tissue (7, 13). Guida et al. observed hemorrhage, edema, and abnormal endothelial cells in the brains and spinal cords of C57BL/6 mice that were infected with wt MAV-1 (11). These pathological findings are likely the cause of the clinical signs of disease and eventual death of the animals.

The functions of gp11K and the other MAV-1 E3 proteins are not known. The gene products of E3 are involved in the pathogenesis of MAV-1 (2), canine adenovirus type 1 (8, 15), and hAds (9, 22, 23). The 50% lethal dose (LD_{50}) values of MAV-1 E3 mutants are higher than those of wt virus, indicating that the E3 mutant viruses are less virulent than wt virus (2, 5). For these reasons, we were interested in designing and constructing an MAV-1 virus null for the expression of E3 proteins. Previous attempts to construct MAV-1 E3 null mutants by mutating the initiator methionine codons to leucine codons were unsuccessful (2, 5). We showed that one of these mutants, *pm*E312, synthesizes E3 gp11K at low levels from an alternatively spliced late transcript as a fusion between a late protein and gp11K (5). It is likely that the other initiator codon mutant (2) also expresses gp11K at late times by the same mechanism, but this has not been experimentally confirmed.

* Corresponding author. Mailing address: Department of Genetics, University of Georgia, Life Sciences Bldg., Athens, GA 30602-7223. Phone: (706) 542-8395. Fax: (706) 542-3910. E-mail: spindler@arches.uga.edu.

† Present address: Southeast Poultry Research Laboratory, ARS/USDA, Athens, GA 30605.

We report here that the insertion of premature termination codons in all three reading frames of the MAV-1 E3 common coding region results in an E3 null mutant, *pm*E314. The virus growth characteristics in cell culture and mice are reported, and the characteristics of *pm*E314 histopathology are described. In situ hybridization was used to determine the role of E3 gene products in the tropism of the virus. The relevance of these findings is discussed.

MATERIALS AND METHODS

Cells and viruses. 3T6 cells were maintained in Dulbecco modified Eagle medium (DMEM) supplemented with 5% heat-inactivated calf serum (HICS). IE3.3 cells were maintained in DMEM supplemented with 8% HICS and 200 μg/ml G418 (5). Mouse brain microvascular endothelial cells (MBMEC) were maintained in MBMEC growth medium (Cell Applications, Inc., San Diego, Calif.). *pm*E101 is a wt virus that contains a single *Eco*RI site in the E3 region (2). It behaves as wt virus in all assays to date and is referred to as wt throughout this work. Using the method to construct viral mutants previously described (2, 4), *pm*E314 was constructed as follows. pBHC-2, a plasmid encoding the MAV-1 *Hin*dIII-C fragment (2), was mutated by using oligonucleotide site-directed mutagenesis (Stratagene). Mutagenic sense and antisense oligonucleotides were designed to incorporate termination codons in all three reading frames at the gp11K signal sequence cleavage site (nucleotide 1149) (numbering scheme is for the MAV-1 *Hin*dIII-C fragment; accession number M30594 [18]). The sequences for the mutagenic oligonucleotides are E3MUTSTOP1 (sense), 5′-G ACC GGT CA**T GAG CTC TAA TAT TTG** ATA TCA TCG CAG TGT-3′, and E3MUTSTOP2 (antisense), 5′-ACA CTG CGA TGA TAT CAA ATA TTA GAG CTC ATG ACC GGT C-3′; for the sense strand boldface indicates the mutagenic termination codons, and the underlined regions show unique restriction sites incorporated to screen for mutants. pMUT-STOP, the resulting mutagenized plasmid, was then linearized and cotransfected (10) into IE3.3 cells with *pm*E101 DNA-protein complex that had been digested with *Eco*RI and partially filled in by using Klenow (2). Plaques resulting from homologous recombination between viral DNA and pMUT-STOP were assayed for the desired mutations by PCR amplification followed by restriction digestion (2). Two independent isolates (*pm*E314 and *pm*E315) were obtained, and sequence analysis (*fmol* DNA Sequencing System; Promega) was performed by PCR amplification of viral DNAs prepared by the Hirt method (12). Surprisingly, the plasmid pMUT-STOP was found to have two copies of the mutagenic oligonucleotide incorporated in tandem. Accordingly, both mutant viruses have six termination codons, two in each reading frame. Analysis of *pm*E314 is presented in this work.

Cell labeling and immunoprecipitation. 3T6 cells were mock, wt, or *pm*E314 infected at a multiplicity of infection (MOI) of 1. Media containing 1% HICS was added to infected cells after a 1-h adsorption period. The cells were radiolabeled with 30 μCi of [^{35}S]cysteine per ml for 4 h prior to harvest. Samples were harvested at 20 h postinfection (hpi; early time point) and 40 hpi (late time point) as previously described (3, 5). After being labeled, samples were adjusted to 2×10^6 trichloroacetic acid-precipitable cpm and immunoprecipitated as previously described. α-Eall3, which recognizes an epitope common to all three E3 proteins (2), and α-E3-1, which recognizes an epitope unique to the E3 gp11K protein (3), were used to immunoprecipitate E3 proteins. To evaluate early and late protein synthesis in wt- and *pm*E314-infected cells, E1A protein was immunoprecipitated with AKO 7-147 (21), and virion proteins were immunoprecipitated with AKO 1-68 as previously described (5, 13). Immunoprecipitated samples were separated by electrophoresis on a 10 to 18% gradient polyacrylamide-sodium dodecyl sulfate gel and visualized by using a PhosphorImager (Molecular Dynamics).

Virus one-step growth curves. 3T6 and MBMECs were mock, wt, or *pm*E314 infected at an MOI of 5. Virus was allowed to adsorb for 1 h at 37°C. The cells were then washed with 1× phosphate-buffered saline three times to remove unadsorbed virus. Virus was harvested at 1 to 5 days postinfection (dpi) by scraping the cells into the media and freeze-thawing the resulting stocks three times. Cell debris was removed from the stocks by centrifugation. The titer of the virus stocks from each time point was determined by plaque assay on IE3.3 cells.

LD_{50} determinations in mice. Tenfold serial dilutions of wt (10^1 to 10^{-3} PFU; the particle/PFU ratio for MAV-1 is 1,000:1) and *pm*E314 (10^6 to 10^1 PFU) viruses were made in conditioned DMEM medium containing 5% HICS. Experiments were carried out in male NIH Swiss outbred mice (Harlan Sprague-Dawley) housed in microisolator cages with food and water supplied ad libitum. The LD_{50} value was determined by injecting intraperitoneally (i.p.) five mice per virus dilution with 100 μl of the dilution. Three mice were mock infected with 100 μl of conditioned medium alone by i.p. injection. The infected mice were monitored twice daily for signs of disease and death. Moribund mice were euthanized by inhalation of CO_2. The LD_{50} value was determined using the method of Reed and Muench (19).

Infection of mice for pathology studies. Male NIH Swiss outbred mice (Harlan Sprague-Dawley) were infected with wt or *pm*E314 viruses by i.p. injection. Mice were infected with virus diluted in conditioned cell culture medium; mock-infected mice received conditioned medium alone. Mice were infected with 10^3 or 10^4 PFU of either wt or *pm*E314 virus. Organs were harvested from mice infected with 10^3 PFU of wt or *pm*E314 virus at 3, 5, 7, 8, 9, and 10 dpi (n = three each day). Organs were collected from mice infected with 10^4 PFU of wt or *pm*E314 virus at 3, 4, 5, 6, and 7 dpi (n = three each day). Organs were taken from mock-infected mice at 3 dpi prior to dissection of infected animals. Mice were euthanized by CO_2 inhalation just prior to necropsy.

Histopathology. Immediately after euthanasia, the following organs were collected in 10% neutral buffered formalin: brain, spinal cord, spleen, thymus, prefemoral and mandibular lymph nodes, intestinal Peyer's patches, kidney, and lung. Tissues were fixed in formalin for 24 h and then embedded in paraffin. Sections were cut routinely for hematoxylin and eosin staining and for in situ hybridization.

In situ hybridization. A 714-nucleotide antisense digoxigenin-labeled riboprobe corresponding to the E3 region (but overlapping with pVIII) of MAV-1 was prepared. In situ hybridization was performed as described previously (13). Briefly, 20 ng of labeled probe was hybridized overnight at 52°C with deparaffinized tissue sections predigested with proteinase K. The following day, sections were subjected to stringent washes, and detection was accomplished with anti-digoxigenin-alkaline phosphatase and with nitroblue tetrazolium and bromcresylindolylphosphate as chromogen and substrate, respectively. Sections were counterstained lightly with hematoxylin and coverslipped with Permount for a permanent record.

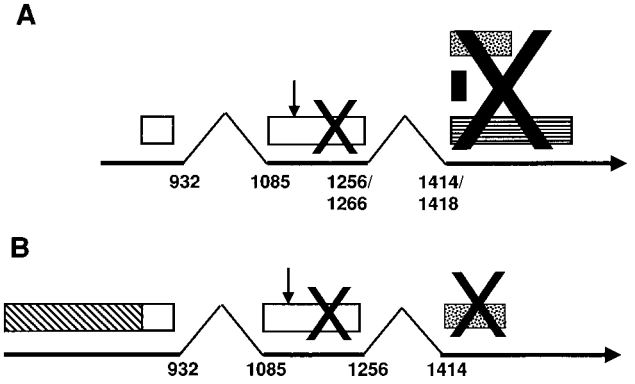

FIG. 1. Schematic diagram of E3 mutagenesis. Early E3 mRNA structure is depicted in panel A and the predicted mRNA from which gp11K is also produced at late times is depicted in panel B (5). Lines indicate mRNA, and carets denote spliced introns. Numbers below the introns indicate splice junctions based on the MAV-1 *Hin*dIII-C fragment numbering system (1, 18). Boxes indicate protein coding regions where a late protein (likely pVIII) (5) is represented by diagonal hatch marks and the common coding region of E3 is indicated by the open boxes. The unique portions of the E3 proteins are as follows: stippling, gp11K protein; solid black, class 2 protein; horizontal stripes, class 3 protein. The known signal sequence cleavage site is marked by a downward arrow. The mutant virus described here, *pm*E314, has termination codons inserted into the E3 common coding region around the signal sequence cleavage site. These mutations are predicted to prevent the translation of the E3 protein sequences (noted by large "X"s) downstream of the signal sequence cleavage site from both early (A) and late (B) mRNAs.

RESULTS

Construction of *pm*E314. Since MAV-1 E3 gp11K is synthesized from a DNA replication-dependent late mRNA in addition to an early mRNA transcribed from a nearby promoter, mutations in the E3 initiator codons do not prevent gp11K protein production (5). Therefore, it was necessary to design a mutation that would prevent protein expression from both early and late E3 mRNAs. We constructed a virus with termination codons in the second exon of the common coding region of E3 (Fig. 1). These termination codons were inserted in all three reading frames and situated around the signal sequence cleavage site. This site was chosen for mutagenesis because this portion of E3 does not overlap with any other known coding regions in MAV-1. The signal peptide is likely to be degraded after cleavage and thus inactive in infected cells, and no mature E3 proteins should be produced due to translational termination. This mutation was first made in a plasmid, pBHC-2, by using oligonucleotide site-directed mutagenesis. After inser-

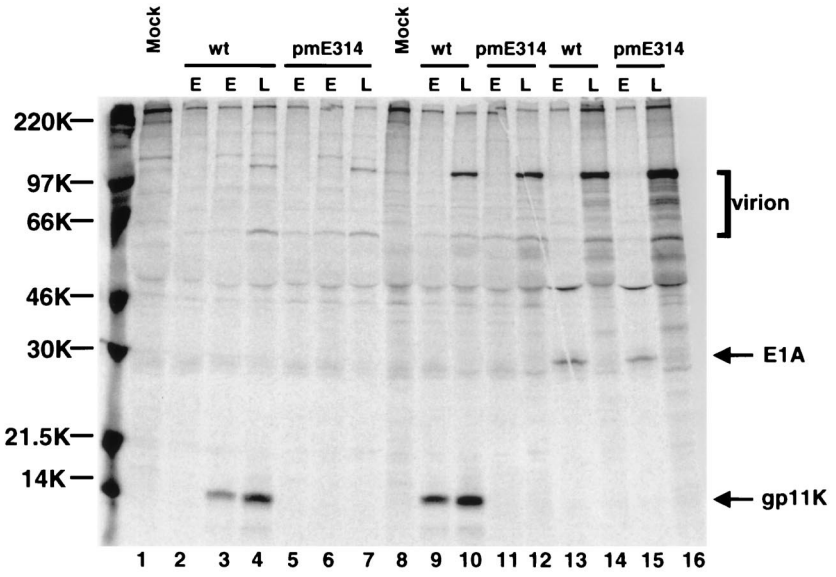

FIG. 2. Immunoprecipitation of MAV-1 proteins. Cells were radiolabeled with [^{35}S]cysteine, and cell lysates were immunoprecipitated with preimmune serum (lanes 2 and 5); α-Eall3 antiserum, which recognizes an epitope common to all three E3 proteins (lanes 1, 3, 4, 6, and 7); and α-E3-1 antiserum, which recognizes the unique portion of gp11K (lanes 8 to 12). E1A protein was immunoprecipitated with AKO 7-147 in lanes 13 and 15. MAV-1 virion proteins were immunoprecipitated with AKO 1-68 in lanes 14 and 16. A protein size standard is noted to the left. Expected sizes of immunoprecipitated proteins are noted to the right.

tion of the termination codons was confirmed by sequence analysis, the mutated plasmid and *pm*E101 DNA-protein complex were cotransfected into IE3.3 cells. Mutant viruses were isolated from plaques and sequencing confirmed that they contained the expected mutations. The mutant virus characterized here is designated *pm*E314.

Since the E3 region of MAV-1 is overlapped by pVIII and closely flanked by fiber, Northern analysis was employed to determine whether the mutations introduced into *pm*E314 affected the steady-state levels of pVIII and fiber messages. Northern analysis revealed that steady-state levels of pVIII and fiber messages in *pm*E314-infected cells were comparable to those of wt virus (data not shown). This result indicates that the mutations introduced into *pm*E314 did not adversely affect pVIII and fiber messages, similar to results seen for other mutations in E3 (2). Furthermore, early E3 messages from *pm*E314-infected cells were absent at early times and accumulated in lower amounts at late times when compared to wt-infected cells (data not shown). Since introduction of premature termination codons into coding regions can cause destabilization of mRNA (16), this result was not surprising.

Altered protein synthesis of *pm*E314-infected cells. To determine whether *pm*E314 synthesized E3 proteins, mock-, wt-, and *pm*E314-infected cells were radiolabeled with [^{35}S]cysteine, and the lysates were immunoprecipitated with two E3 antisera. α-Eall3 antiserum recognizes an epitope common to all three E3 proteins (2), and α-E3-1 antiserum recognizes the unique C-terminal portion of gp11K (3). E3 proteins were not immunoprecipitated from mock-infected cell lysates with either E3 antiserum (Fig. 2, lanes 1 and 8), nor were E3 proteins immunoprecipitated with preimmune serum from wt- or *pm*E314-infected cell lysates (Fig. 2, lanes 2 and 5). The α-Eall3 antiserum immunoprecipitated gp11K from wt-infected cell lysates at both early and late times postinfection, and class 2 and class 3 proteins were not detected, as previously described (2) (Fig. 2, lanes 3 and 4). E3 proteins were not immunoprecipitated from *pm*E314-infected cell lysates at early or late times in infection, as expected (Fig. 2, lanes 6 and 7).

Similar results were obtained with the α-E3-1 antiserum. gp11K was immunoprecipitated at early and late times from wt-infected cell lysates (Fig. 2, lanes 9 and 10) (3), and gp11K was not detected in *pm*E314-infected cell lysates (Fig. 2, lanes 11 and 12). To ensure that expression of other early and late proteins was not affected by the mutations introduced into *pm*E314, E1A and virion proteins were immunoprecipitated from wt- and *pm*E314-infected cell lysates. Levels of these proteins were comparable in wt- and mutant-infected cell lysates, indicating that early and late protein synthesis was not affected by mutations in the E3 region (Fig. 2, lanes 13 and 15 for E1A and lanes 14 and 16 for virion proteins). A slight difference in E1A levels was observed in wt- and *pm*E314-infected cells in this particular experiment (Fig. 2, lanes 13 and 15) and was likely due to minor loading differences. These results indicate that *pm*E314 is null for the expression of MAV-1 E3 proteins and that the mutations in *pm*E314 specifically affect E3 expression.

MAV-1 E3 is dispensable in cell culture. One-step growth curves were used to compare the growth of *pm*E314 in vitro to that of wt virus. Both viruses were grown on mouse 3T6 fibroblasts (the cell line we standardly use to propagate virus) and MBMECs. Since wt MAV-1 infects endothelial cells in vivo, particularly those in the brain and spinal cord (13), we chose MBMECs as a cell line with biological relevance to the animal system. Both 3T6 and MBMEC cells were infected with wt and pmE314 viruses and were harvested daily for 5 dpi (Fig. 3). In 3T6 cells the titer at 5 dpi was 4.5×10^6 PFU/ml with a standard deviation of 8.3×10^5 for wt virus, and 4.6×10^6 PFU/ml with a standard deviation of 2.0×10^6 for *pm*E314 virus (Fig. 3A). *pm*E314 grew to titers similar to that of wt virus at other time points that were measured. Similar results were obtained when wt and *pm*E314 were grown on MBMECs. At 5 dpi in MBMECs, wt virus grew to a titer of 3.4×10^6 PFU/ml with a standard deviation of 2.1×10^6. *pm*E314 grew to a titer of 3.6×10^6 PFU/ml with a standard deviation of 1.4×10^6 (Fig. 3B). At other time points measured, *pm*E314 and wt virus grew to similar titers. These results show that *pm*E314 grows equally well and with similar kinetics to wt in both 3T6 and

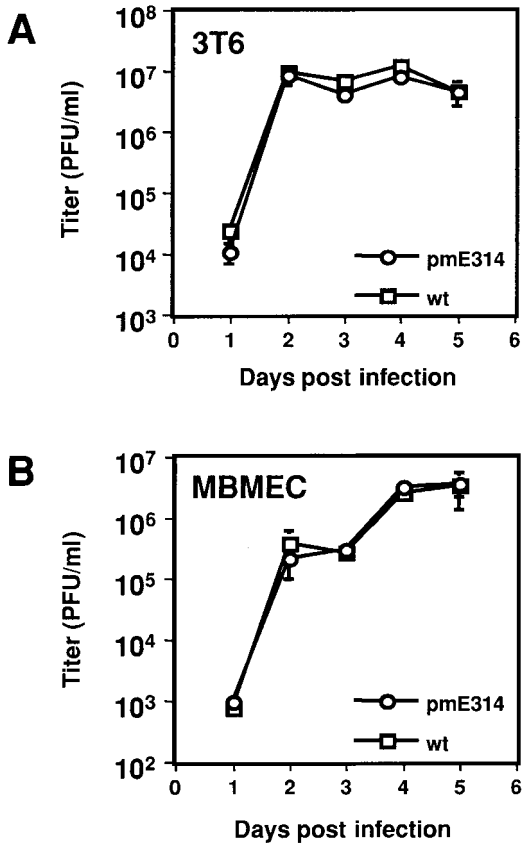

FIG. 3. Growth curve analysis of wt- and *pm*E314-infected mouse cells. 3T6 cells (A) and MBMECs (B) were infected with wt and mutant viruses at an MOI of 5. Infections were harvested, and virus yields were determined by plaque assay on IE3.3 cells.

MBMEC cells, indicating that the E3 proteins are dispensable for growth in the cultured cell lines tested.

***pm*E314 is less virulent than wt virus in NIH Swiss outbred mice.** LD_{50} values were determined for wt and *pm*E314 viruses in NIH Swiss outbred mice by i.p. injections of 10-fold serial dilutions of virus into mice. The LD_{50} value for wt was $10^{-1.5}$ PFU (~30 particles; the MAV-1 particle/PFU ratio is 1,000:1), which is consistent with LD_{50} values determined by others (Table 1) (2, 14, 20). The LD_{50} value for *pm*E314 averaged $10^{5.5}$ PFU (Table 1). This represents a difference in LD_{50} values of approximately 6 log units. These results clearly indicate that the absence of E3 proteins alters the virulence of the virus in NIH Swiss outbred mice. Viral DNA was PCR amplified from the spleens of *pm*E314-infected animals, and the resulting PCR products were sequenced. All samples contained the expected mutations (data not shown).

The *pm*E314-infected mice were monitored twice daily for signs of disease, and we found that when these mice exhibited clinical disease, the signs were consistent with those observed for wt-infected mice, i.e., ruffled coat, mild ataxia, and hunched posture and posterior paresis, followed by total flaccid paralysis and abdominal breathing. As in wt-infected mice, the onset of clinical signs of disease was also dose dependent in *pm*E314-infected mice. Mice infected with 10^6 PFU of *pm*E314 died peracutely without observed clinical signs of disease at 3 or 4 dpi. Mice infected with 10^5 PFU showed signs of disease previously reported and died at 5 to 9 dpi. Mice infected at lower doses showed no overt clinical signs of disease and did not die. Histopathology of mice infected with 10^5 or 10^6 PFU of *pm*E314 showed little endothelial damage but did show multiple adenovirus inclusion bodies. These mice had extensive positive staining as seen by in situ hybridization, indicating that they likely died from infection of an overwhelming number of cells (data not shown). These results show that *pm*E314 virus did not alter the clinical signs of disease that were manifested in the infected mice and that the onset of disease was dose dependent.

Striking differences in histopathology of wt- and *pm*E314-infected mice. In the mice given 10^3 or 10^4 PFU of wt virus, histopathologic changes were similar in character at both doses but differed in time of onset. The most significant findings were in the brain and spinal cord. With the 10^3 dose, by 5 and 7 dpi, there was evidence of degeneration of central nervous system (CNS) capillary endothelium, with mild fragmentation of endothelial cell cytoplasm, and increased prominence of nuclei. At this time, there was pavementing and margination of inflammatory cells in these CNS capillaries. By 8 and 9 dpi, vessel walls were thickened, with various degrees of mural invasion, occasional microhemorrhage, and the formation of fibrin thrombi in rare capillaries (Fig. 4A). At 10 dpi, mural invasion was still evident in some capillaries, and focal areas of early cortical necrosis were evident.

With 10^4 PFU of wt virus, CNS changes were evident slightly earlier, at 4 dpi, and consisted of perivascular edema. By 5 dpi, mural invasion and fibrinoid necrosis of vascular walls was widespread. Microhemorrhage and thrombosis were evident at 6 and 7 dpi.

In contrast, in mice given 10^3 PFU of *pm*E314 virus, no histopathologic changes were observed in brain until 8 and 9 dpi, when there was some degeneration of CNS capillary endothelial cytoplasm, with minimal pavementing of inflammatory cells (Fig. 4B). In the mice sacrificed at 10 dpi, the endothelial cell walls appeared slightly "plump," but otherwise there were no signs of reactivity. In mice given 10^4 PFU of *pm*E314 virus, some perivascular edema was seen around CNS capillaries at 4 dpi. At 6 and 7 dpi, there was continued perivascular edema and degeneration of vessel walls, but unlike wt infection, neither pavementing of inflammatory cells nor mural invasion was observed.

The only other significant histopathologic change noted in the mice was the formation of germinal centers in the spleen of mice infected with both wt and mutant viruses (data not shown). Other tissues that were examined were normal. In the mice given wt virus, this occurred at 9 dpi with the 10^3 PFU dose and at 6 dpi with the 10^4 PFU dose. For the *pm*E314 virus-infected mice, germinal center formation was noted at 8 dpi with the 10^3 PFU dose and 7 dpi with the 10^4 PFU dose (data not shown).

Similar in situ hybridization staining for wt- and *pm*E314-infected mice. Patterns of staining were similar in the paired dosage groups, indicating that mutation of the E3 region did not alter the tropism of the virus (Fig. 4C and D; Tables 2 and 3). The greatest amounts of viral nucleic acid were detected in

TABLE 1. LD_{50} determination of *pm*E314 and wt viruses in NIH Swiss outbred mice

Virus	LD_{50} (log PFU)[a]			
	Expt 1	Expt 2	Expt 3	Avg
*pm*E314	5.2	5.9	4.6	5.5
wt	ND	ND	−1.5	

[a] Particle/PFU ratio = 1,000:1. ND, not determined.

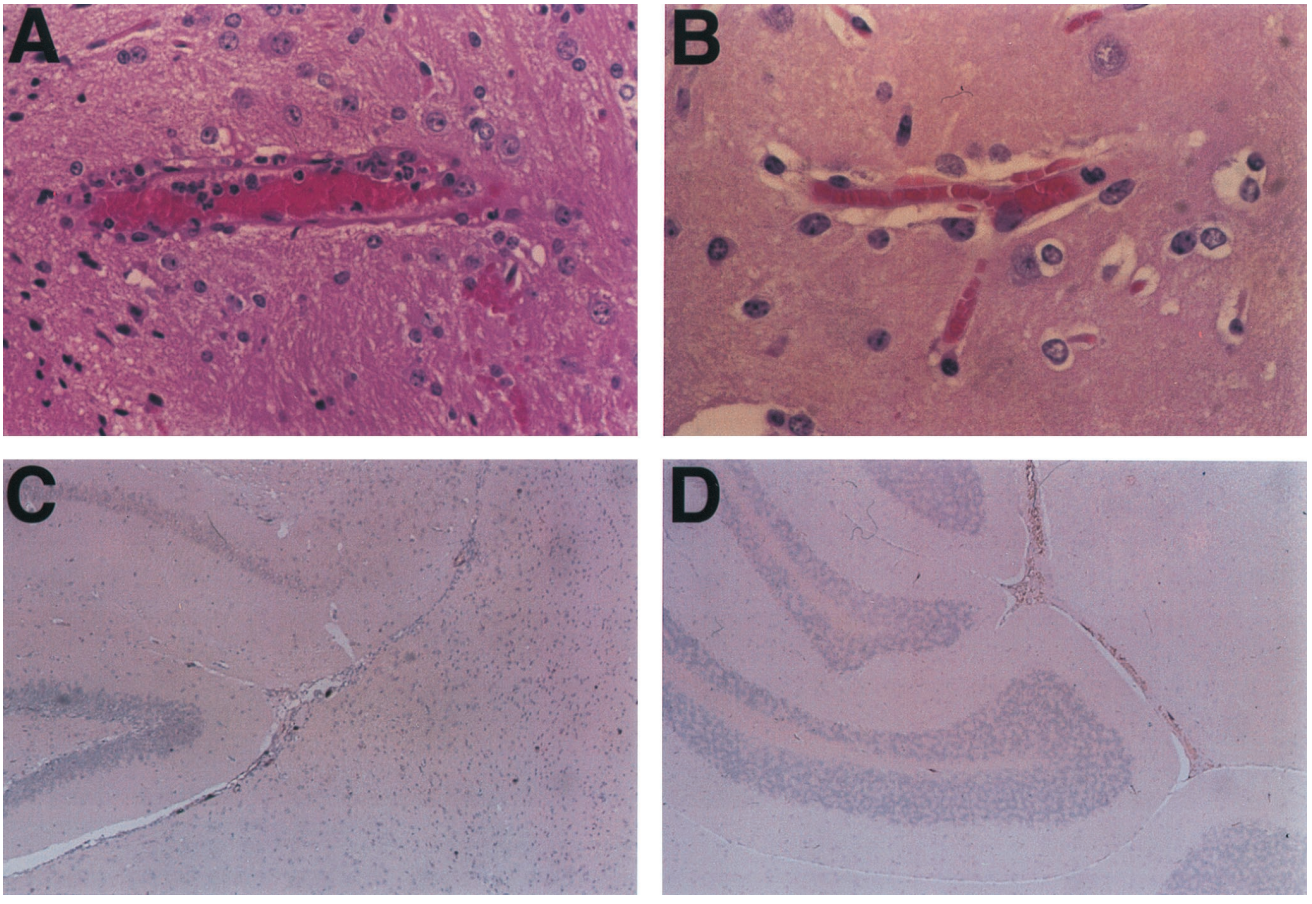

FIG. 4. Effects of virus infection of mouse tissues. Histopathology of brain from adult outbred Swiss mice infected with 10^3 PFU of wt (A) or pmE314 (B) viruses at 8 dpi is shown. Histopathology damage is more extensive in wt-infected mice (see text for details). In situ hybridization of brain samples from adult outbred Swiss mice infected with 10^4 PFU of wt (C) or *pm*E314 (D) virus at 6 dpi is shown. Cells positive for in situ hybridization with a MAV-1 E3/pVIII probe in C and D were observed as dark brown staining. Vascular endothelial staining was seen in both wt and mutant virus-infected tissue; greater amounts were seen in wt-infected tissue at this dosage. Magnification, ×316, ×395, ×79, and ×79 (panels A to D, respectively).

brain and spinal cord. In the mice given 10^3 PFU inoculating dose, positive staining was seen as early as 8 dpi with the wt virus (all three mice) and at 7 dpi with the *pm*E314 virus-infected mice (one of three mice). The extent of staining was similar as well, with fairly diffuse capillary staining noted in both groups given 10^3 PFU virus at 8 dpi. By 10 dpi, there were some differences in that with the mice given wt virus, there was still evidence of infection in numerous capillaries in all three mice, whereas in the mice given *pm*E314 virus, capillary infection at this time point was rare and was seen in only one of three mice. In contrast, in the two groups given 10^4 PFU virus, there was earlier and more widespread evidence of viral nucleic acid (Fig. 4C and D). The viral nucleic acid was visualized as positive staining of capillary endothelium at 3 dpi with the wt virus and at 4 dpi with *pm*E314 virus. The wt virus-infected mice had greater numbers of capillaries affected per high-power field than did mutant virus-infected mice.

Positivity in the spleen was strongest with the 10^4 PFU dose for both wt and mutant viruses and was visualized as individual cell staining in red pulp. The positive cells were morphologi-

TABLE 2. In situ hybridization staining for MAV-1 E3 and pVIII nucleic acid in tissues from mice infected with wt or *pm*E314 virus at a 10^3 PFU inoculating dose

Virus	Organ	Staining at[a]:					
		3 dpi	5 dpi	7 dpi	8 dpi	9 dpi	10 dpi
wt	Brain and spinal cord	− (3/3)	− (3/3)	− (3/3)	+++ (3/3)	++ (2/3)	+++ (3/3)
	Spleen	− (3/3)	− (3/3)	− (3/3)	++ (2/3)	− (3/3)	+ (1/3)
*pm*E314	Brain and spinal cord	− (3/3)	− (3/3)	+ (3/3)	+++ (3/3)	++ (3/3)	+ (1/3)
	Spleen	− (3/3)	− (3/3)	+ (1/3)	+++ (1/3)	+ (2/3)	+ (1/3)

[a] −, No staining seen in any of the tissues examined; +, infrequent staining (0 to 1 positive cell per high-power field [×100]); ++, regular staining (approximately 1 positive cell per high-power field); +++, extensive staining (more than 1 positive cell per high-power field). The number of mice for which this level of staining was observed/number of mice examined is shown in parentheses.

TABLE 3. In situ hybridization staining for MAV-1 E3 and pVIII nucleic acid in tissues from mice infected with wt or *pm*E314 viruses at a 10^4 PFU inoculating dose

Virus	Organ	Staining at[a]:				
		3 dpi	4 dpi	5 dpi	6 dpi	7 dpi
wt	Brain and spinal cord	++ (3/3)	++ (3/3)	+++ (3/3)	+++ (3/3)	+++ (3/3)
	Spleen	++ (3/3)	+ (1/3)	+++ (2/3)	++ (2/3)	+ (2/3)
*pm*E314	Brain and spinal cord	− (3/3)	+ (2/3)	++ (3/3)	++ (2/3)	++ (2/3)
	Spleen	− (3/3)	− (3/3)	++ (3/3)	+ (2/3)	− (3/3)

[a] −, No staining seen in any of the tissues examined; +, infrequent staining (0 to 1 positive cell per high-power field [×100]); ++, regular staining (approximately 1 positive cell per high-power field); +++, extensive staining (more than 1 positive cell per high-power field). The number of mice for which this level of staining was observed/number of mice examined is shown in parentheses.

cally compatible with being endothelium and stationary macrophages.

DISCUSSION

We have constructed the first MAV-1 E3 null mutant, *pm*E314. Multiple termination codons were inserted into the E3 coding region, and in cells infected by *pm*E314, E3 proteins were not detected in infected cell lysates by immunoprecipitation with two different E3 antisera (Fig. 2). This result was supported by Northern analysis that showed that steady-state levels of E3 mRNAs were greatly reduced in *pm*E314 infections compared to those of wt virus (data not shown). Previous attempts to design a null mutant had been unsuccessful and revealed that MAV-1 E3 gp11K is synthesized from a late mRNA (2, 5). The mutagenesis strategy utilized here prevented protein expression from both the early and late E3 mRNAs.

The clinical signs of disease observed for *pm*E314 infections were the same as those previously reported for wt virus in NIH Swiss outbred mice (14). *pm*E314 also exhibited a dose-dependent onset of clinical signs of disease. However, clinical signs of disease were seen in mice given 10^5 or 10^6 PFU but not in those given 10^3 or 10^4 PFU of *pm*E314. Histopathology and in situ hybridization of tissues collected from mice infected with 10^5 and 10^6 PFU of *pm*E314 showed characteristics different from those of a wt infection. It is likely that these doses overwhelmed the normal operation of the endothelial cells of the brain and spinal cord, resulting in high numbers of infected cells throughout these tissues.

When mice infected with 10^3 or 10^4 PFU of *pm*E314 were evaluated, no clinical signs of disease or death were observed and the histopathology showed strikingly different characteristics from those of wt virus at equivalent doses. The *pm*E314-infected mice exhibited only minimal endothelial damage and lacked the inflammatory response observed in brains and spinal cords of wt-infected mice. However, the in situ hybridization results showed similar patterns of viral nucleic acid distribution in both wt- and *pm*E314-infected mice, with slightly less staining in the mutant-infected mice (Tables 2 and 3; Fig. 4C and D). These findings suggest that *pm*E314 replicates similarly to wt virus in mice but does not cause the same degree of cell damage or recruitment of inflammatory cells to the site of infection. This hypothesis is supported by growth curve analysis in vitro in both 3T6 mouse fibroblasts and MBMECs (Fig. 3), where wt and *pm*E314 viruses grow to comparable titers at comparable rates.

Since *pm*E314-infected cells do not efficiently recruit inflammatory cells in vivo, it is likely that an E3 product is responsible in some way for this action. Results from studies with other MAV-1 E3 mutant viruses suggest that gp11K may be important in this process (2, 5). Other E3 mutants that have been studied have the ability to produce only one of the three E3 proteins (2). The most profound effect on LD_{50} among those mutants is seen in the viruses in which gp11K is absent but which retain the ability to make the E3 class 2 or class 3 proteins (2). The LD_{50} value for *pm*E314 (null for all three E3 proteins: gp11K, class 2, and class 3) is higher than that of the mutants lacking only gp11K (Table 1; see also reference 2). This indicates that it is likely that all three E3 proteins play a role in the pathogenesis of the virus in mice.

The functions of MAV-1 E3 proteins are not known; thus, it is difficult to speculate on a direct or indirect mechanism by which E3 proteins affect the recruitment of inflammatory cells to wt MAV-1-infected endothelium. However, a few general possibilities exist. It is possible that, lacking the E3 proteins, *pm*E314 simply does not replicate in vascular endothelium as well as wt virus. This explanation is unlikely since growth curve analysis showed that *pm*E314 grew to titers comparable to those of wt virus in MBMECs, indicating that *pm*E314 can infect and replicate well in cells derived from vascular endothelium. There was also abundant evidence of MAV-1 nucleic acid in CNS endothelium in *pm*E314-infected mice as determined by in situ hybridization. Another possibility is that E3 proteins may be good targets for recognition by the immune system and, in their absence, the immune response is lower and thus tissue damage is below the threshold required to cause disease. Inada and Uetake reported T-cell recognition of MAV-1 antigen(s) produced at early times in infection, but unfortunately these antigens were not identified (12a). The recruitment of inflammatory cells to the site of infection by wt MAV-1 may be an indirect result of some (unknown) function of the E3 proteins. For example, an E3 function may inadvertantly cause cell damage that attracts inflammatory cells to the infection site. Alternatively, the E3 proteins may interact more directly with or upregulate some component of the immune response, causing the recruitment of the inflammatory cells. Recently, IP-10/crg-2, a multifunctional chemokine that promotes recruitment of inflammatory cells to endothelium, was shown to be upregulated in the CNS and spleens of C57BL/6 mice infected with wt MAV-1 (6). This factor is upregulated in the MAV-1-susceptible C57BL/6 mouse strain but not in the resistant BALB/c mice. It is unknown if this factor is a general marker for MAV-1-susceptible mice or what role, if any, it plays in determining this susceptibility. Since the NIH Swiss mice used in our study are susceptible to MAV-1 infection (14), it is possible that IP-10/crg-2 is upregulated in these mice infected with wt MAV-1. If so, it would be interesting to determine the levels and the mechanism of IP-10/crg-2 upregulation in both wt- and *pm*E314-infected mice.

Although E3 is the most divergent region of the adenovirus

genome, it has retained a role in the pathogenesis of adenoviruses throughout its evolutionary history. Like the E3 gene products of MAV-1, those of hAds and canine adenovirus type 1 (CAV-1) are dispensable in cell culture but are involved in the pathogenesis of the viruses (this work; see also references 2, 8, 9, and 22). Compared to wt hAd viruses, infection with mutants with deletion of two of the three hAd E3 genes that protect infected cells from tumor necrosis factor alpha results in an increase in inflammation in cotton rats and more severe disease in mice (9, 22). In contrast, when E3 mutants of CAV-1 and MAV-1 are evaluated in dogs or mice, respectively, the mutations result in viruses that are less virulent than wt in vivo (this work; see also references 2, 5, and 8). In particular, the MAV-1 E3 null mutant causes less inflammation than wt (Fig. 4A, B). Although the E3 proteins of CAV-1 and MAV-1 both affect the virulence of their respective viruses, they exhibit no sequence similarity.

This study is the first pathological survey of an MAV-1 E3 null mutant in vivo. We found significant differences in the ability of wt and E3 null mutant viruses to recruit inflammatory cells to the site of infection. This confirms previous results that the MAV-1 E3 gene products are involved in the pathogenesis of MAV-1 (2, 5) and suggests that the E3 products either directly or indirectly recruit inflammatory cells to infected endothelium. However, the mechanism that promotes this recruitment remains unclear. Work is under way to determine the general mechanism that causes the difference in histopathology between wt and *pm*E314 viruses, as well as the function of the MAV-1 E3 gene products.

ACKNOWLEDGMENTS

We are grateful to Melissa Scott, Gwen Hirsch, Emily Smith, and Adriana Kajon for technical assistance and to Adriana Kajon, Rich Meagher, Lois Miller, and Kelley Moremen for comments on the manuscript. We thank Dave Brown for computer assistance. We thank Howard Fox (Scripps Research Institute) for the generous gift of MBMECs.

This work was supported by NIH grant AI23762 and American Cancer Society grant VM-176 to K.R.S. and by NIH predoctoral traineeship (GM 07103) to A.N.C.

REFERENCES

1. **Beard, C. W., A. O. Ball, E. H. Wooley, and K. R. Spindler.** 1990. Transcription mapping of mouse adenovirus type 1 early region 3. Virology **175:**81–90.
2. **Beard, C. W., and K. R. Spindler.** 1996. Analysis of early region 3 mutants of mouse adenovirus type 1. J. Virol. **70:**5867–5874.
3. **Beard, C. W., and K. R. Spindler.** 1995. Characterization of an 11K protein produced by early region 3 of mouse adenovirus type 1. Virology **208:** 457–466.
4. **Cauthen, A. N., and K. R. Spindler.** 1999. Construction of mouse adenovirus type 1 mutants, p. 85–103. *In* W. S. M. Wold (ed.), Adenovirus methods and protocols. Humana Press, Totowa, N.J.
5. **Cauthen, A. N., and K. R. Spindler.** 1999. Novel expression of mouse adenovirus type 1 early region 3 gp11K at late times after infection. Virology **259:**119–128.
6. **Charles, P. C., X. Chen, M. S. Horwitz, and C. F. Brosnan.** 1999. Differential chemokine induction by the mouse adenovirus type-1 in the central nervous system of susceptible and resistant strains of mice. J. Neuro virol. **5:**55–64.
7. **Charles, P. C., J. D. Guida, C. F. Brosnan, and M. S. Horwitz.** 1998. Mouse adenovirus type-1 replication is restricted to vascular endothelium in the CNS of susceptible strains of mice. Virology **245:**216–228.
8. **Dragulev, B. P., S. Sira, M. G. AbouHaidar, and J. B. Campbell.** 1991. Sequence analysis of putative E3 and fiber genomic regions of two strains of canine adenovirus type 1. Virology **183:**298–305.
9. **Ginsberg, H. S., U. Lundholm-Beauchamp, R. L. Horswood, B. Pernis, W. S. M. Wold, R. M. Chanock, and G. A. Prince.** 1989. Role of early region 3 (E3) in pathogenesis of adenovirus disease. Proc. Natl. Acad. Sci. USA **86:** 3823–3827.
10. **Gorman, C., R. Padmanabhan, and B. H. Howard.** 1983. High efficiency DNA-mediated transformation of primate cells. Science **221:**551–553.
11. **Guida, J. D., G. Fejer, L.-A. Pirofski, C. F. Brosnan, and M. S. Horwitz.** 1995. Mouse adenovirus type 1 causes a fatal hemorrhagic encephalomyelitis in adult C57BL/6 but not BALB/c mice. J. Virol. **69:**7674–7681.
12. **Hirt, B.** 1967. Selective extraction of polyoma DNA from infected mouse cell cultures. J. Mol. Biol. **26:**365–369.

12a. **Inada, T., and H. Uetake.** 1977. Virus-induced specific cell surface antigen(s) on mouse adenovirus-infected cells. Infect. Immun. **18:**41–45.

13. **Kajon, A. E., C. C. Brown, and K. R. Spindler.** 1998. Distribution of mouse adenovirus type 1 in intraperitoneally and intranasally infected adult outbred mice. J. Virol. **72:**1219–1223.
14. **Kring, S. C., C. S. King, and K. R. Spindler.** 1995. Susceptibility and signs associated with mouse adenovirus type 1 infection of adult outbred Swiss mice. J. Virol. **69:**8084–8088.
15. **Linné, T.** 1992. Differences in the E3 regions of the canine adenovirus type 1 and type 2. Virus Res. **23:**119–133.
16. **Maquat, L. E.** 1995. When cells stop making sense: effects of nonsense codons on RNA metabolism in vertebrate cells. RNA **1:**453–465.
17. **Meissner, J. D., G. N. Hirsch, E. A. LaRue, R. A. Fulcher, and K. R. Spindler.** 1997. Completion of the DNA sequence of mouse adenovirus type 1: sequence of E2B, L1, and L2 (18–51 map units). Virus Res. **51:**53–64.
18. **Raviprakash, K. S., A. Grunhaus, M. A. El Kholy, and M. S. Horwitz.** 1989. The mouse adenovirus type 1 contains an unusual E3 region. J. Virol. **63:** 5455–5458.
19. **Reed, L. J., and H. Muench.** 1938. A simple method of estimating fifty per cent endpoints. Am. J. Hyg. **27:**493–497.
20. **Smith, K., C. C. Brown, and K. R. Spindler.** 1998. The role of mouse adenovirus type 1 early region 1A in acute and persistent infections in mice. J. Virol. **72:**5699–5706.
21. **Smith, K., B. Ying, A. O. Ball, C. W. Beard, and K. R. Spindler.** 1996. Interaction of mouse adenovirus type 1 early region 1A protein with cellular proteins pRb and p107. Virology **224:**184–197.
22. **Sparer, T. E., R. A. Tripp, D. L. Dillehay, T. W. Hermiston, W. S. Wold, and L. R. Gooding.** 1996. The role of human adenovirus early region 3 proteins (gp19K, 10.4K, 14.5K, and 14.7K) in a murine pneumonia model. J. Virol. **70:**2431–2439.
23. **Tufariello, J., S. Cho, and M. S. Horwitz.** 1994. The adenovirus E3 14.7-kilodalton protein which inhibits cytolysis by tumor necrosis factor increases the virulence of vaccinia virus in a murine pneumonia model. J. Virol. **68:** 453–462.